AFRL-SR-BL-TR-98-

0460

Report Documentation Page

Public reporting burden for this collection of information is estimated to average 1 hour per response, including the time for reviewing instructions, searching existing data sources, gathering and maintaining the data needed, and completing and reviewing the collection of information. Send comments regarding this burden estimate or any other aspect of this collection of information, including suggestions for reducing this burden, to Washington Headquarters Services, Directorate for Information Operations and Reports, 1215 Jefferson Davis Highway, Suite 1204, Arlington, VA 22202-4302, and to the Office of Management and Budget. Paperwork Reduction Project (0704-0188), Washington DC 20503.

1. AGENCY USE ONLY *(Leave blank)*	2. REPORT DATE	3. REPORT TYPE AND DATES COVERED	
	5/4/98	Final Report	08/15/97 - 02/14/98

4. TITLE AND SUBTITLE

Novel Organic Polymer Films for Real-time Holographic Processing

5. FUNDING NUMBERS

C: F29620-97-C-0051

6. AUTHOR(S)

James E. Millerd

7. PERFORMING ORGANIZATION NAME(S) AND ADDRESS(ES)

MetroLaser, Inc.
18010 Skypark Circle #100
Irvine, CA 92614-6428

8. PERFORMING ORGANIZATION REPORT NO.

TBO1JMF.DOC

9. SPONSORING/MONITORING AGENCY NAME(S) AND ADDRESS(ES)

Dr. Charles Y-C. Lee
AFOSR/NE Directorate of Chemistry and Life Sciences
110 Duncan Ave., Room B115
Bolling AFB, DC 20332-8050

10. SPONSORING/MONITORING AGENCY REPORT NUMBER

11. SUPPLEMENTARY NOTES

12a. DISTRIBUTION/AVAILABILITY STATEMENT

Approved for public release; distribution is unlimited

12b. DISTRIBUTION CODE

A

16. Abstract

This Phase I STTR was to develop and commercialize new technologies based on state-of-the-art photorefractive organic polymer films recently developed at the University of Arizona. During Phase I emphasis was placed on developing an optical device that can perform fast, high resolution, whole field (imaged), profile measurements of three-dimensional (3D) objects. A breadboard system was constructed that could be switched between a digital holographic arrangement and a real-time holographic interferometer which incorporated the photopolymer. A number of objects were measured and the best results were obtained with the digital holographic arrangement. A multi-wavelength processing algorithm was implemented to process the discontinuous changes in height of the objects. The profile measurements had a resolution of 80 microns in the z direction and was limited by the tuning range of the laser diode. For future systems the resolution is expected to be improved down to 0.4 microns. The fast unwrapping of discontinuous fringes across the object was a major milestone for the Phase I research. The quantitative 3D measurement system has numerous commercial applications in the aerospace, manufacturing and medical industries.

14. SUBJECT TERMS

Photorefractive Photopolymer Profilometry Holography

15. NUMBER OF PAGES

16

16. PRICE CODE

17. SECURITY CLASSIFICATION OF REPORT	18. SECURITY CLASSIFICATION OF THIS PAGE	19. SECURITY CLASSIFICATION OF ABSTRACT	20. LIMITATION OF ABSTRACT
Unclassified	Unclassified	Unclassified	SAR

DTIC QUALITY INSPECTED 4

19980602 039

Final Report

Novel Organic Polymer Films for Real-Time Signal Processing

STTR Phase I

8/15/97-2/14/98

James E. Millerd
MetroLaser
18010 Skypark Circle
Suite 100
Irvine, Ca 92614

http://www.metrolaserinc.com

Table of Contents

1. PROGRAM SUMMARY

The University of Arizona has recently developed organic polymer films with outstanding properties for photonic applications.[1] The organic polymers have superior characteristics compared with inorganic crystals and can be uniquely tailored. Parameters such as photogeneration, transport, and electro-optic activity can be controlled *independently* in polymers, making it possible to optimize them for a wide variety of applications. In addition, polymers can be manufactured at a lower cost than inorganic crystals and can easily be fabricated as wide area films. MetroLaser has been developing several commercial instruments based on real-time holography including profilometers for measuring the 3-D shape of diffuse reflecting objects, optical correlators for security applications, and resonant holographic interferometry systems for measuring species concentration in combustion and spray environments. The project teamed researchers at the University of Arizona with MetroLaser scientists to develop and commercialize novel optical instrumentation based on the use of the new organic polymer films.

The period of performance began on August 15, 1997. On August 26th, MetroLaser scientists, James Millerd and Neal Brock, met with University of Arizona researchers, Nasser Peyghambarian and Bernard Kippelen, to review the program goals. It was agreed that several samples would be designed and fabricated for operation at 800 nm.

During the Phase I research, the application of 3-D profilometry was studied. Performance requirements for the polymers were outlined based on system modeling. The University of Arizona fabricated, measured, and delivered several polymer films to MetroLaser. The thickness of all the samples was 105 μm and the polymer was sandwiched between two transparent indium-tin oxide (ITO) electrodes. At 830 nm, a maximum of η_{max} = 74% diffraction efficiency was observed in samples at an applied field of 60 V/μm.

A breadboard system was constructed to measure the three-dimensional shape of diffuse reflecting objects based on multi-wavelength holography. Software was written, tested, and debugged to acquire and process multi-wavelength interferogram contour data. The breadboard could be switched between a digital holographic arrangement and a real-time holographic interferometer by moving a piezo-electric mirror and introducing the photorefractive polymer. The scattering level in the polymer was found to limit the range of object reflectivities that could be measured. The digital holographic arrangement produced the best results in terms of resolution and object reflectivity that could be measured.

A number of objects, including a wedge-shaped object, was measured with the breadboard system (see Figure 1). The multi-wavelength processing algorithm was successfully able to process the discontinuous changes in step height of the objects. The profile data had a resolution of 80 microns in the z direction and was limited by the tuning range of the laser diode. For future systems the resolution is expected to be improved down to 0.4 microns. The fast unwrapping of discontinuous fringes across the object was a major milestone for the Phase I research.

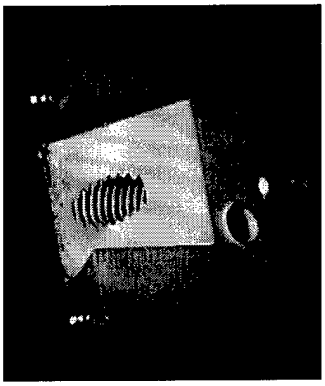

a)

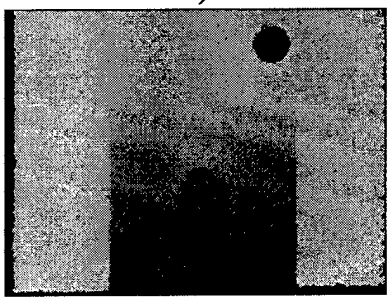

b)

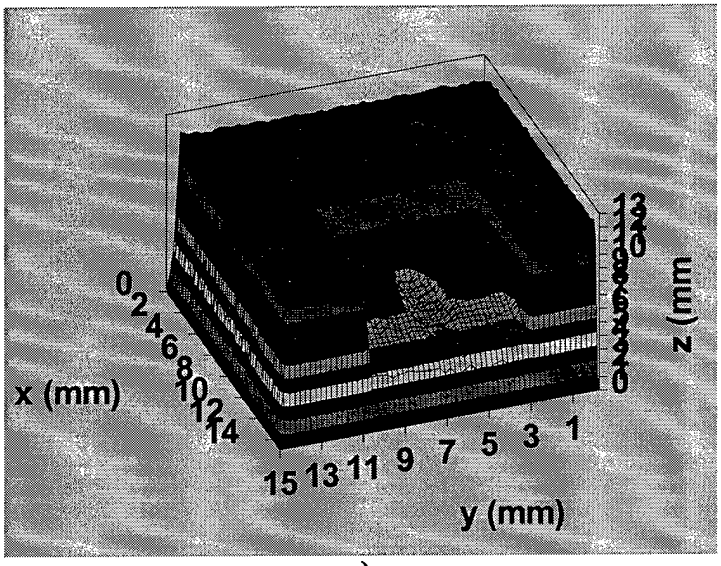

c)

Figure 1. a) Image of wedge object. b) Grayscale contour map of wedge produced using the multi-wavelength breadboard. Note that discontinuity of the hole is profiled. c) 3-D plot of profile data.

2. BACKGROUND AND PROGRAM OBJECTIVES

A fundamental problem in modern optical technology is the fabrication of low cost, high performance non-linear optical materials for switching, modulation, frequency conversion, and real-time holography. Inorganic crystals have traditionally been used for these applications but are less than ideal in terms of cost, performance, and durability. The University of Arizona has recently developed organic polymer films with outstanding properties for photonic applications. The organic polymers have superior characteristics compared with inorganic crystals and can be uniquely tailored. Parameters such as photogeneration, transport, and electro-optic activity can be controlled *independently* in polymers, making it possible to optimize them for a wide variety of applications. In addition, polymers can be manufactured at a lower cost than inorganic crystals and can easily be fabricated as wide area films. These polymers show tremendous potential for use as modulators, switches, optical data storage media, and real-time holographic materials.

MetroLaser, a small business that specializes in the design and development of state-of-the-art optical instrumentation, has been developing a technique for measuring the 3-D profile of opaque objects utilizing inorganic crystals for real-time holographic interferometry. The best crystals currently available are adequate for demonstration purposes but limit commercialization of the instrument because of their high cost, slow response at infrared wavelengths, and fragile nature. This Phase I project teamed researchers at the University of Arizona with MetroLaser scientists to develop an optical profilometer based on the use of the new organic polymer films.

The principle of the measurement is to interfere two images of an object illuminated by different wavelengths. A non-linear optical material is necessary to holographically store one or both of

the images so that they can be interfered. The resulting interference pattern corresponds to planes of constant elevation and thus, the three-dimensional profile of an object can be measured. The resolution of the measurement can be adjusted by controlling the difference in wavelengths and rapid parallel image processing can be accomplished by employing multiple wavelengths. By using a tunable laser diode, which can be tuned rapidly and continuously, and a photorefractive photopolymer material, which has high efficiency and low cost, a compact and robust instrument can be manufactured.

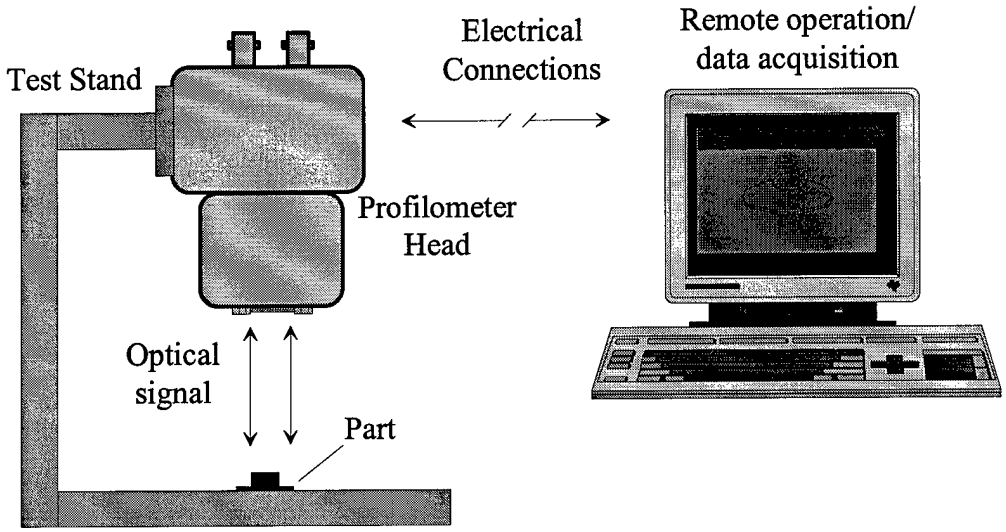

Figure 2. Conceptual design of real-time profilometer system for inspection of parts.

Three-dimensional profile measurements are of fundamental interest in a wide variety of fields including aerospace, manufacturing, and medicine. Accurate measurement of profiles can permit inspection of wear, quality assurance, and automated replication of components. For example, one-of-a-kind or out of production parts on an aircraft can be quickly reproduced, dental crowns can be machined to identically match a tooth using superior materials that are not compatible with existing casting methods, and critical components for high cost machinery can be checked prior to installation to avoid costly failures. Figure 2 shows how the instrument could be used as an optical profilometer for parts inspection. Current 3-D measurement systems utilizing a contacting probe are slow, expensive and very large, thus preventing their widespread use. Current non-contacting 3-D measurement instruments require the operator to map out the object point-by-point which is slow and tedious. The real-time holographic instrument offers fast, non-contacting measurement capability at a much lower cost than current systems. Therefore, a significant commercial marketplace exists for the proposed instrument. In addition, the improved organic polymers have many other commercial applications that could be developed in the future.

The objective of the Phase I research was to demonstrate that a low cost, robust measurement system could be developed using the organic polymers developed at the University of Arizona and the profilometer technology developed at MetroLaser.

The approach used to achieve this objective included the following elements:

- Take advantage of the tailorability and processability of organic materials to optimize existing photorefractive polymers for use in the profilometer system.
- Demonstrate real-time acquisition of profilometry data using organic polymers as the photorefractive recording medium.
- Validate software coding of the image processing algorithm using numerical simulation.
- Demonstrate reduction of real-time images using new software.
- Estimate measurement accuracy and resolution for Phase II prototype.

2.1. Measurement Methodology

The measurement method uses a photorefractive material for real-time coherent optical signal processing. The basic optical arrangement is shown in Figure 3. Using a mono-static configuration, a coherent beam illuminates the target and scattered light is collected. The scattered light is mixed with a reference beam at the Fourier plane to record phase information in the photorefractive polymer material. The laser wavelength is then scanned quickly over discrete steps at the video frame rate. The CCD camera detects the coherent interference between the reconstructed wave from the polymer and the real-time wave coming from the target. This interference produces a modulation of the intensity at each pixel. The basic equation for the intensity at each pixel is given by

$$I_n(x,y) = A(x,y) + B(x,y)\cos\left(\frac{4\pi\Delta\lambda_n}{\lambda^2}\left(C(x,y) + R(x,y)\right)\right), \quad (1)$$

where A and B are constants that depend on the scattered light intensity and efficiency of the non-linear optical material, C is a constant that depends on the exact configuration used inside the instrument, R is the range to the target, λ is the nominal laser wavelength, and $\Delta\lambda$ is the change in wavelength. The process can be thought of as interferometry using a synthetic wavelength given by $\lambda^2/\Delta\lambda$. By collecting multiple images, each with a different laser (or synthetic) wavelength, the scattered light intensity can be factored out and the absolute target profile can be calculated. The precision and range of the measurement is controlled by the choice of the wavelength steps. Initially small steps are used to produce large synthetic wavelengths which can measure over large distances but with poor resolution. The steps are made increasingly larger to increase resolution of the measurement.

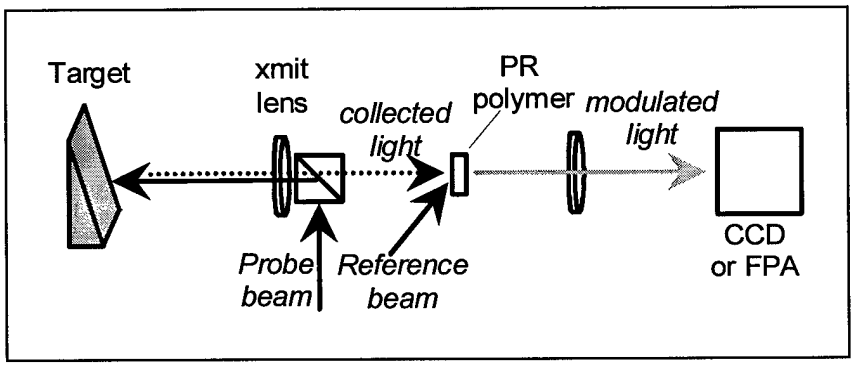

Figure 3. Basic optical layout for multi-wavelength imaging profilometer.

It is important to note that the measurement is made on a pixel-by-pixel basis. Unlike conventional interferometry, which uses information from neighboring pixels to calculate relative phase (in a process known as phase unwrapping), the absolute phase at each pixel is calculated independently. Thus, the system acts as a range detector with N parallel channels, where N is the number of camera pixels. The parallel nature of the measurement lends itself to fast parallel processing architectures so that acquisition and calculation of range across an entire image can be performed extremely fast.

2.2. Photorefractive Polymers

A photorefractive material must possess photosensitivity at the wavelengths well below the energy gap (i.e., not strongly absorbed inside the medium), it must be photoconductive, yet insulating in the dark, and it should possess electro-optic properties. This combination of properties in a single compound is rather rare and, until recently, the choice of photorefractive materials was almost exclusively confined to inorganic electro-optic crystals (e.g., $LiNbO_3$). Over the past few years photorefractive polymers have rapidly emerged as an alternative to inorganic photorefractive crystals.[2,3] In contrast to inorganic materials, the three basic processes responsible for hologram formation, photogeneration, transport, and electro-optic activity, can be optimized *independently* in polymers. This unique feature, together with the rich structural flexibility of organic materials, offers great opportunities for further improvement of these materials. Moreover, photorefractive polymers offer new properties such as molecular orientation by the periodic, internal space-charge field, field-dependent photogeneration efficiency, and field-dependent mobility. These properties are ideal for applications in real-time holographic signal processing.

The Arizona group has recently synthesized a polymer with a gain coefficient of $\Gamma > 200$ cm^{-1}, four times higher than that of the best photorefractive inorganic crystal to date ($BaTiO_3$: $\Gamma = 50$ cm^{-1}). Reversible refractive index modulations as high as $\Delta n = 10^{-2}$ can be induced with mW laser diodes in a guest/host system based on the photoconductive polymer host poly(N-vinylcarbazole) (PVK). This result establishes that polymeric materials can exhibit photorefractive efficiencies far in excess of inorganic crystals. Most likely, it is attributed to the significantly smaller dielectric constant of the polymers and much larger density of the photosensitive centers,[3] but it is still the subject of active research. Simultaneously, polymers have several other important advantages over traditional crystals, including lower cost, better processing characteristics, and availability as a wide area thin film. These features significantly improve the operation and commercial potential of the profilometer system.

3. PHASE I RESULTS

3.1 Photorefractive Photopolymer Fabrication and testing

The photorefractive (PR) polymer composite developed at The University of Arizona for this program was based on the chromophore DHADC-MPN (2-N,N-dihexylamino-7-dicyanomethylidenyl-3,4,5,6,10-pentahydronaphthalene). The molecule was used as a dopant molecule in mixtures of poly(N-vinylcarbazole) (PVK) and N-ethylcarbazole (ECZ). Sensitivity

in the near IR was provided by (2,4,7-trinitro-9-fluorenylidene) malonitrile (TNFDM). The PR properties, in particular the dynamic range, or Δn, were tested by four-wave mixing experiments in the tilted geometry. The thickness of all the samples was 105 μm and the polymer was sandwiched between two transparent indium-tin oxide (ITO) electrodes. Two-beam coupling, i.e., energy exchange between the two interfering laser beams, was observed and confirmed the PR nature of the optical encoding. At 830 nm, a maximum of η_{max} = 74% diffraction efficiency was observed in samples of the composite DHADC-MPN:PVK:ECZ:TNFDM (25:49:25:1 wt. %) at an applied field of 60 V/μm. The normalized diffraction efficiency versus applied field for p- and s-polarized read-out is a sample with composition DHADC-MPN:PVK:ECZ:TNFDM (25:49:24:2 wt. %) is shown in Figure 4.

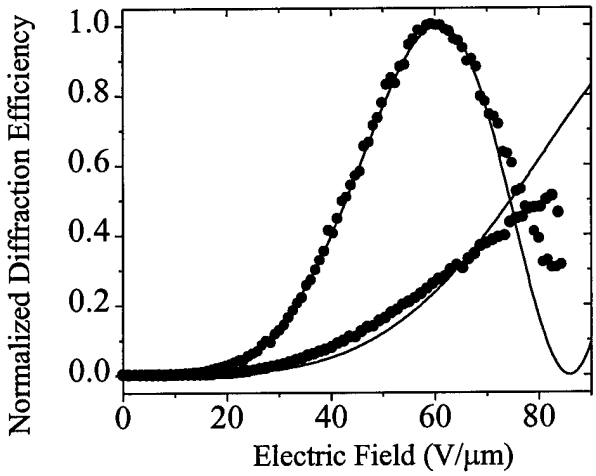

Figure 4. Measured diffraction efficiency for a 100 micron polymer film (U of A). Lower diffraction efficiency is for s polarized light.

Measurements were made on one of the polymers samples at MetroLaser. The experimental arrangement is shown in Figure 5. An 800 nm laser was used for two beam coupling measurements and to write the grating in four wave mixing experiments. A 780 nm laser was used to read out the grating in the four wave mixing experiments. After several hours of use at 6.5 kV several of the samples experienced dielectric breakdown. Table 1 shows the measured gain which was smaller than that measured at the University of Arizona and possibly due to differences in laser intensity.

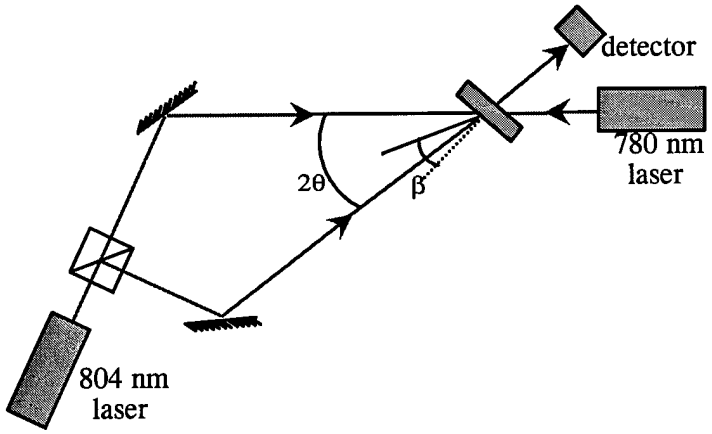

Figure 5. Experimental arrangement for measuring photopolymer performance at 804 nm

Table 1.

Measured gain coefficients in photopolymers at 804 nm. (2θ = 30 deg, β = 45 deg)

Applied field V/micron	Gain coefficient cm^{-1}	Calculated Diffraction efficiency %
40	14	.1
44	14	.1
50	19	.2
55	38	.9
60	91	5.2
65	103	6.7

The gain coefficient was also measured as a function of beam ratio (reference to object). Figure 6 shows the measured beam coupling gain as a function of beam ratio. The gain was not corrected for pump depletion. The scattering floor was measured at 2000:1 for the F#20 system used. The measured scattering floor increased significantly for the lower F# system used in imaging.

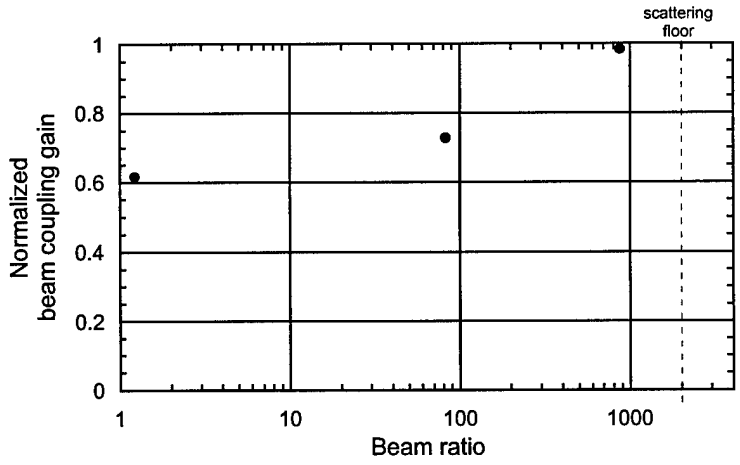

Figure 6. Normalized beam coupling gain as a function of beam ratio. Scattering floor was measured at 2000:1 for an F#20 system.

The necessary diffraction efficiency for the photopolymer was calculated as a function of object reflectivity and laser power (shown in Figure 7). The primary factor influencing this calculation was CCD sensitivity. The reflectivity of several types of objects was measured using an F#6 system. Based on the measurements and calculations, the diffraction efficiency of the photopolymer should be adequate to measure even black plastic objects with a 30 mW laser diode. Unfortunately the scattering floor for the polymer material limited its use with weakly reflecting objects. The scattering floor of the polymer was measured to be 0.5% for the F#6 system which was well above the raw reflectivity of white painted objects, and a factor of 4 below the retroreflective paint. The scattering floor turned out to limit the usefulness of the polymer during Phase I.

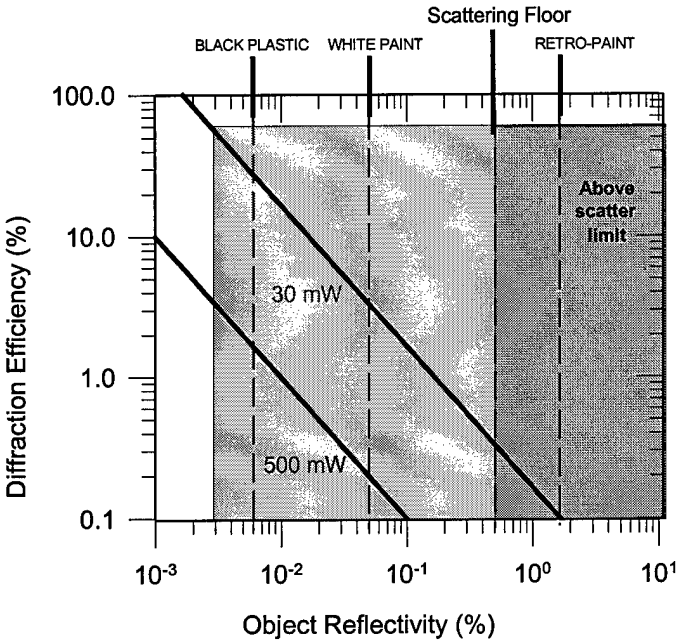

Figure 7. Calculated diffraction efficiency necessary as a function of object reflectivity and laser power. Also plotted is the raw reflectivity of several objects as well as the scattering floor for the polymer material using an F#6 collection system.

3.2 Software Development

A significant portion of the Phase I program was devoted towards developing a multi-wavelength algorithm for processing discontinuous changes in object height. This development is very crucial since the processing of discontinuous phase maps has limited the wide scale development of holographic measurement systems in the past.

For this project two different processing algorithms were analyzed; real-time phase shift holographic interferometry and digital holography. In holographic interferometry, a hologram is written in the photorefractive material, then the laser is quickly tuned to a new wavelength and four images are captured each with a phase shift of $\pi/2$ (induced by a moving mirror). Holographic interferometry is characterized by a uniform modulation on each pixel and zero

phase offset. Because of the uniformity, the range can be found by processing only four frames of data. Each pixel of the four images can be represented by

$$I_n(x,y) = A(x,y)\left[1 + B\cos\left(\frac{4\pi\Delta\lambda}{\lambda^2}R(x,y) + \frac{n\pi}{2}\right)\right], \tag{2}$$

where n = 0,1,2,3. The target range can be found using the following transformation

$$R(x,y) = \frac{\lambda^2}{4\pi\Delta\lambda}\tan^{-1}\left(\frac{I_3(x,y) - I_1(x,y)}{I_0(x,y) - I_2(x,y)}\right). \tag{3}$$

Thus, four frames of data can be used to measure distance.

The digital holographic method requires eight frames of data; four baseline and four after tuning the laser. It has the advantage of not requiring a real-time photorefractive material but is characterized by a much higher noise level due to fact that each pixel has a random modulation index and phase offset. For the baseline image, the intensity of each pixel is given by

$$Ib_n(x,y) = A(x,y) + B(x,y)\cos\left(\phi(x,y) + \frac{n\pi}{2}\right). \tag{4}$$

After tuning the laser the intensity of each pixel is given by,

$$It_n(x,y) = A(x,y) + B(x,y)\cos\left(\frac{4\pi\Delta\lambda_n}{\lambda^2}R(x,y) + \phi(x,y) + \frac{n\pi}{2}\right), \tag{5}$$

The range can be solved for by combining pixel from the eight images in the following way

$$R(x,y) = \frac{\lambda^2}{4\pi\Delta\lambda}\tan^{-1}\left(\frac{X(x,y)}{Y(x,y)}\right), \tag{6}$$

where

$$X(x,y) = [Ib_3(x,y) - Ib_1(x,y)]*[It_0(x,y) - It_2(x,y)] - [It_3(x,y) - It_1(x,y)]*[Ib_0(x,y) - Ib_2(x,y)]$$
$$Y(x,y) = [Ib_0(x,y) - Ib_2(x,y)]*[It_0(x,y) - It_2(x,y)] + [Ib_3(x,y) - Ib_1(x,y)]*[It_3(x,y) - It_1(x,y)]$$

This algorithm is considerably more computationally intensive than for the case of holographic interferometry (Eqn. 3). Additionally, because of the speckle noise, it is necessary to perform a spatial average over neighboring pixels. This can be accomplished by [4]

$$R(x,y) = \frac{\lambda^2}{4\pi\Delta\lambda}\tan^{-1}\left(\frac{\sum_{x,y\in\delta} X(x,y)}{\sum_{x,y\in\delta} Y(x,y)}\right), \tag{7}$$

where the sums are performed over the range of δ nearest neighbors.

Because of the modelo 2π behavior of the arctangent function, the range is wrapped (ambiguous) beyond the so-called synthetic wavelength

$$\lambda_s = \frac{\lambda^2}{4\pi\,\Delta\lambda}. \tag{8}$$

To resolve this range ambiguity it is possible to use multiple synthetic wavelengths and incrementally add the range distance.[5] The overall range is then given by,

$$R'(x,y) = \sum_m \frac{R_{\Delta\lambda m}(x,y)}{m}, \tag{9}$$

where m is the number of wavelength steps used and $R_{\Delta\lambda m}$ is the range measured with a frequency tuning of $\Delta\lambda/m$. Implied in this method is that no single measurement should have a phase value greater than 2π, which can place a restriction on the maximum size of the object that can be measured.

Software was written, tested, and debugged to acquire and process multi-wavelength interferogram contour data using the algorithms above. The multi-wavelength algorithm was tested using synthetically generated data. In addition, the noise filtering algorithm (Eqn. 9) was developed and tested using the synthetic data. After successful trials with synthetic data, the routines were optimized for speed. The streamlined routines were then incorporated with the video acquisition hardware and used to measure objects on the optical breadboard.

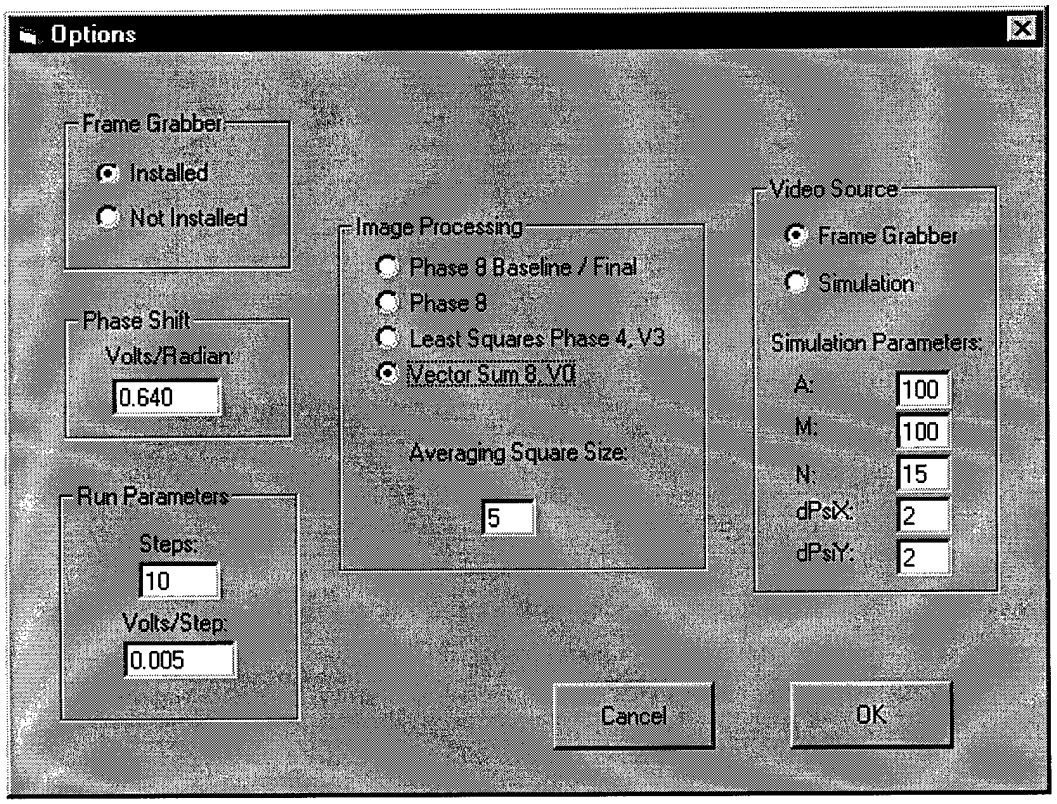

Figure 8. Pop-up options menu allowed testing of each algorithm, simulated or video data, and control of laser tuning steps for multi-frame algorithm.

3.3 Breadboard Design

A breadboard was constructed to acquire profile data and test the multi-wavelength acquisition and processing software. A 30 mW, 800 nm laser diode was used along with a combination of lenses, beamsplitters and mirrors shown in Figure 9. The breadboard could be switched between a digital holographic arrangement and a real-time holographic interferometer by moving the location of the piezo-electric mirror and introducing the photorefractive polymer.

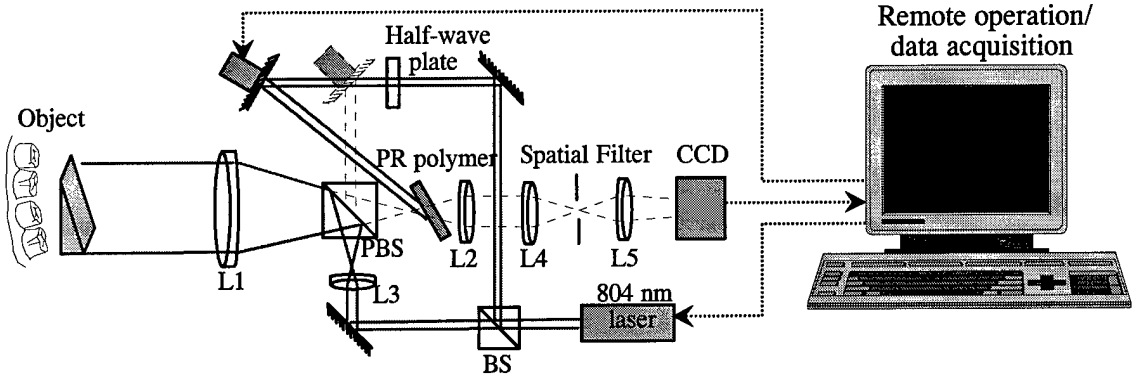

Figure 9. Optical Breadboard for 3D profiling of diffusely reflecting objects.

Component specifications for the breadboard are as follows:

- L1 - Diameter = 50mm, focal length = 100 mm, achromat, NIR anti-reflection coated
- L2 - Diameter = 25mm, focal length = 50 mm, achromat, NIR anti-reflection coated
- L3 - Diameter = 10mm, focal length = 18 mm, plano convex, NIR anti-reflection coated
- L4 - Diameter = 25mm, focal length = 50 mm, achromat, NIR anti-reflection coated
- L5 - Diameter = 25mm, focal length = 50 mm, achromat, NIR anti-reflection coated
- BS - Non polarizing, NIR beamsplitter 50/50 split, NIR anti-reflection coated
- PBS - polarizing beamsplitter, NIR anti-reflection coated
- Laser - 30 mW, single longitudinal mode, 804 nm, 4mm beam diameter, circular

3.4. Profilometry Measurements

A 3-D profile of a wedge shaped object that was measured with the breadboard system is shown in Figure 1 (digital holographic arrangement). The multi-wavelength processing algorithm was successfully able to process the discontinuous changes in step height around the edges of the object and the hole in the upper right corner. The fast unwrapping of discontinuous fringes across the object is a major milestone for the Phase I research.

Figure 10 shows the software interface which includes several options for the acquisition and processing of data. A functional and source code listing of the code is included as Appendix A to this report. Also shown in Figure 10 is a wrapped phase map of the wedge object. Approximately 4 1/2 fringes can be viewed descending the sloped face of the wedge. The image was produced by acquiring a baseline set of four images, tuning the laser diode, and then displaying continuous phase maps. The difficulty of phase unwrapping can be appreciated by observing that the top flat

surface has the same gray scale value as several positions along the sloped surface. This ambiguity is difficult if not impossible for conventional fringe unwrapping algorithms to resolve correctly.

Using the multi-frame algorithm of equation 9 it is possible to unambiguously determine ranges beyond the synthetic wavelength. This was done by automating the tuning of the laser and the acquisition of the video frames. Figure 11 shows the unwrapped image of the wedge after using 10 tuning steps of the laser. Discontinuities at the side of the object as well as the hole and the sloped front were measured. This represents a significant advance over previous interferometric measurement systems since it can process discontinuities and still use on-axis illumination.

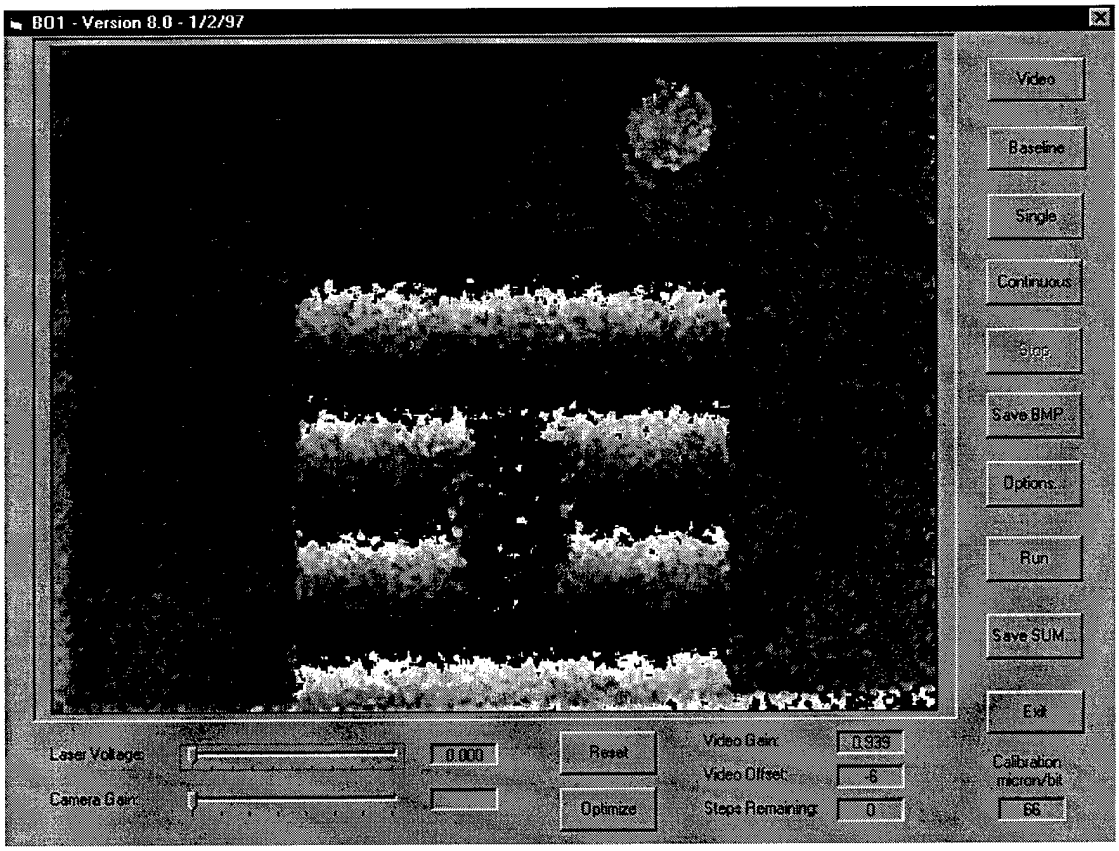

Figure 10. Software display and wrapped phase map of wedge.

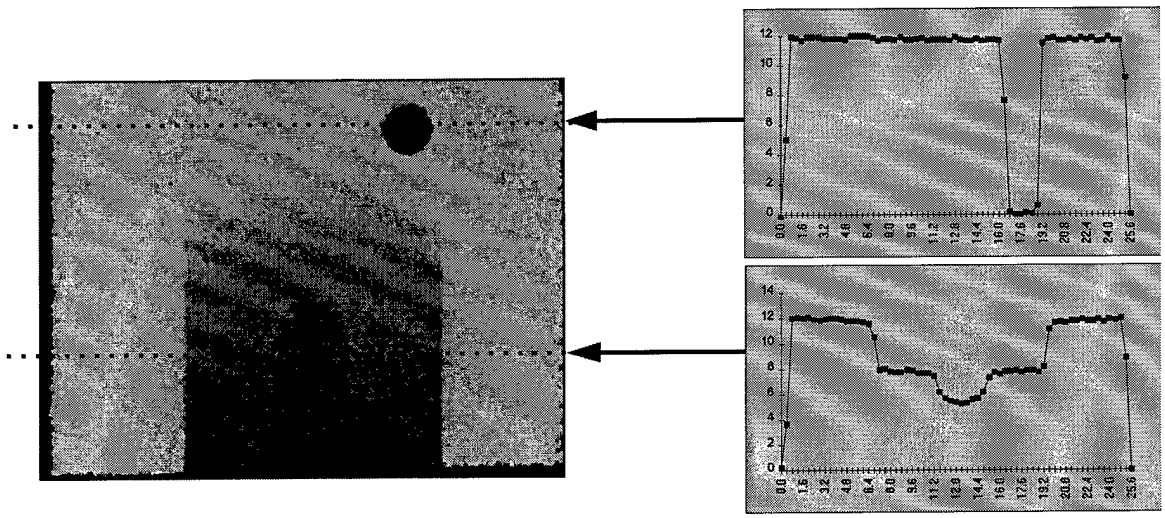

Figure 11. Unwrapped profile data of wedge object. Graphs at right correspond to slices of data across the object as indicated. Note that the system was correctly able to resolve discontinuities in height at the edges, the hole in back, and the sloped surface with respect to the deck height.

The profile data had a resolution of 80 microns in the z direction and was limited by the tuning range of the laser diode. By using a grating tuned laser, the resolution is expected to be improved down to 0.4 microns.

Spatial resolution in the x and y directions was approximately 100 microns and was limited by the field-of-view, number of pixels in the CCD, and the spatial averaging necessary to reduce noise. Figure 12 shows an unwrapped image of wedge without any spatial averaging. The high percentage of drop-out pixels (low modulation) is characteristic of digital holography. Using the algorithm of Eqn. 7, the smooth map of Figure 11 can be produced.

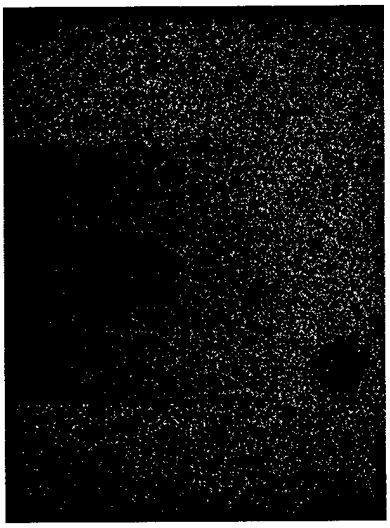

Figure 12. Unwrapped image of wedge without any spatial averaging. The high percentage of drop-out pixels (low modulation) is characteristic of digital holography.

The incorporation of the new photorefractive polymers into the system should greatly improve the spatial resolution of the system by reducing the necessity for spatial averaging. Incorporation of a high density CCD will also improve spatial resolution. A 25 micron spatial resolution for a 1 inch field-of-view is expected.

The system was also used to profile plaster replicas of human teeth (digital holographic arrangement). Figure 13 shows results from two molars. Discontinuous features of the teeth (drop between tooth and gum line) were measured correctly as well as surface features of the tooth. This test confirmed the utility of the measurement technique in the medical and dental fields.

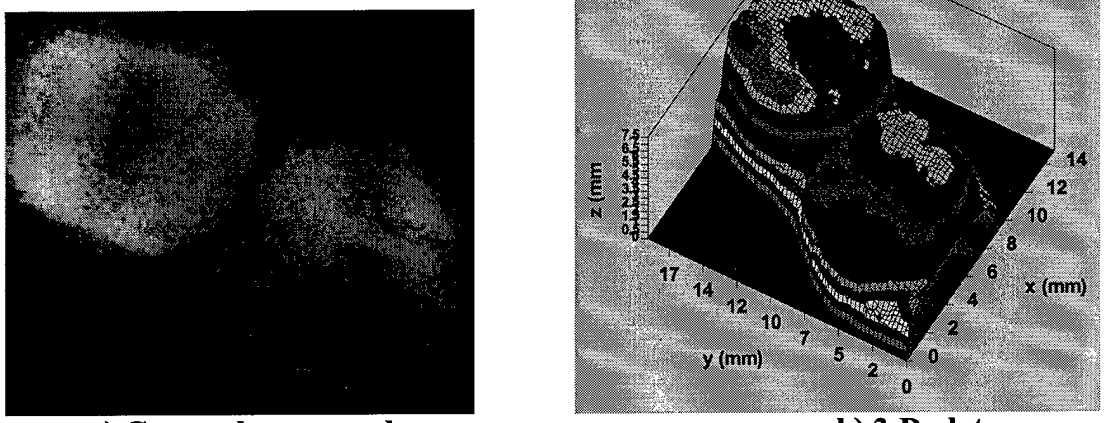

a) Grayscale map, and **b) 3-D plot.**

Figure 13. Contour of plaster replicas of human teeth.

Integration of the photorefractive photopolymer was limited by the scattered noise floor as outlined in 3.1 Photorefractive Photopolymer Fabrication and testing section. This precluded measurement of diffuse reflecting objects; however, it was possible to measure mirrored surfaces and surfaces coated with retro-reflective paint. Figure 14a shows a holographic interferogram of a mirrored surface recorded in the photopolymer material. No filtering was used in this image. Figure 14b shows a multi-frame contour map of turbine blades that were coated with retro-reflective paint. Again, no spatial filtering was used for this image. The greatly improved image quality compared with the unfiltered digital holographic image (Figure 12) exemplifies how the photopolymer material can improve the system spatial resolution. Presently, this enhancement is off-set by the increased scattering floor which prohibits measurement of diffusely reflecting surfaces.

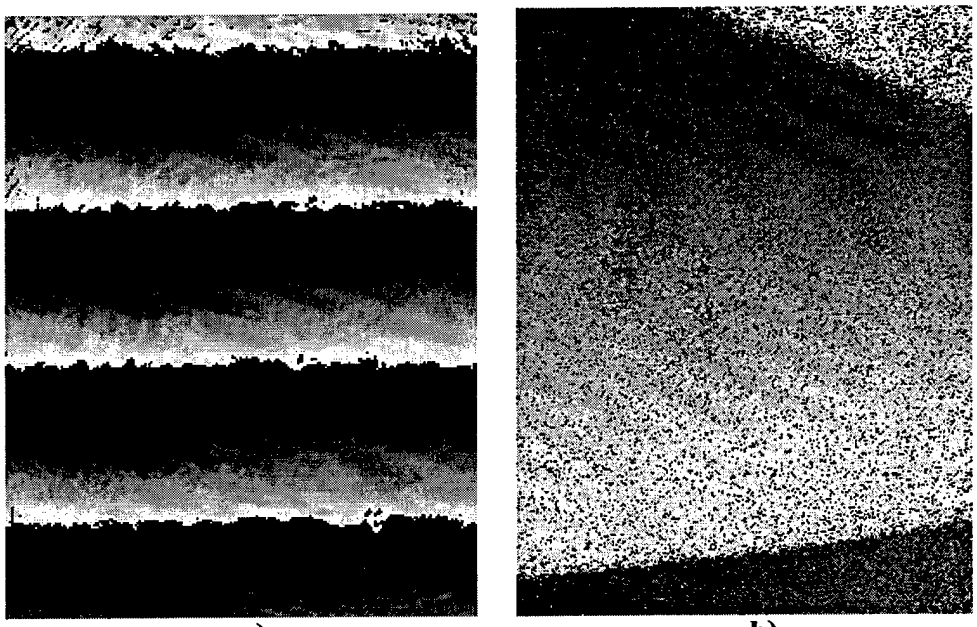

a) b)

Figure 14. a) Holographic interferogram of a mirrored surface and b) turbine blades painted with retro-reflective paint, recorded with photorefractive polymer materials.

4. CONCLUSIONS & RECOMMENDATIONS

The breadboard system was built and successfully contoured objects of approximately 1 inch in diameter. The multi-frame software algorithm was successfully written and debugged. The measurement could be made quickly (30 seconds) and had a resolution of 80 microns in Z, 100 microns in X and Y. The Z resolution was primarily limited due to the small tuning range of laser diode. X and Y resolution were limited by the number of pixels in the CCD and the image field size. The scattering floor of the polymer limited the range of object reflectivity that could be examined.

If this research is continued in the future, the following steps are recommended: 1) optimizing material properties that effect performance including: the reduction of scattering in the polymers, possibly through the use of a different host matrix with better scattering properties, and increasing quantum efficiency, possibly by incorporating a bi-functional dopant (i.e., a chromophore that is responsible for light absorption and birefringence); 2) developing a compact prototype system for fast and accurate measurement; and 3) begin commercialization of the technology by developing manufacturing procedures and establishing partnerships with manufacturing and marketing firms.

5. REFERENCES

1 K. Meerholz, B.L. Volodin, Sandalphon, B. Kippelen and N. Peyghambarian, "A photorefractive polymer with high optical gain and diffraction efficiency near 100%", *Nature* **371**, pp. 497-500 (1994).

2 S. Ducharme, J.C. Scott , R.J. Tweig , W.E. Moerner, *Phys. Rev. Lett.*, **66**, pp. 1846-1849 (1991).

3 W.E. Moerner and S.M. Silence, "Polymeric Photorefractive Materials", *Chem. Rev.* **94**, pp. 127-155 (1994).

4 This is similar to the method described in C.K. Hong, H.S. Ryu, and H.C. Lim, "Least-squares fitting of the phase map obtained in phase-shifting electronic speckle pattern interferometry," Opt. Lett., Vol. 20 No. 8 pp. 931-933 (1995).

5 J.M. Huntley and H.O. Saldner, "Profilometry using temporal phase unwrapping and a spatial light modulator-based fringe projector," Opt. Eng. 36 pp. 610-615 (1997).